Prediction of Low-Frequency Sound Field in Rooms with Complex-Valued Boundary Conditions on Walls

Mirosław MEISSNER
Institute of Fundamental Technological Research, Polish Academy of Sciences, Pawińskiego 5B, 02-106 Warsaw, Poland, mmeissn@ippt.pan.pl

Abstract

A modal representation of a room impulse response has been used to formulate expressions for low-frequency sound field in rooms of arbitrary shape. Based on theoretical results, a simulation program has been developed to predict a sound pressure distribution and a room transfer function for rectangular enclosure having walls covered by a material of complex impedance. Calculation results have shown that changes in the wall reactance entail a substantial modification of a sound pressure distribution. Furthermore, an influence of wall reactance on the room transfer function was investigated and it was discovered that a change in a reactance sign causes a shift in frequencies of modal vibrations excited in the room.

Keywords: room acoustics, modal vibrations, room impulse response, complex wall impedance

1. Introduction

The main objective of theoretical room acoustics is to investigate the steady-state and transient acoustic behaviors of enclosed spaces. There are many theoretical methods for modeling a sound field inside enclosures and among them are diffusion-equation models, geometrical approaches, wave-based methods and modal expansion methods. The diffusion-equation models [1] are an extension of the statistical theory to spatially varying sound field. Geometrical approaches are suitable for high sound frequencies and the ray tracing method [2], the beam tracing algorithm [3] and the mirror source technique [4] are the most popular methods for geometric modeling. In contrast to geometric approaches, wave-based methods provide a complete description the sound field because they solve the wave equation after suitable space discretization. The most common among these numerical techniques are the finite element method [5], the boundary element method [6] and the finite-difference time-domain method [7]. Modal expansion methods yield the acoustic modes of pressure vibrations inside enclosures and the sound field is expressed as a linear combination of these modes [8]. Modal expansion approaches are more difficult to apply for irregularly shaped rooms [9], but they fully describe a wave nature of the sound field like a diffraction and a creation of standing waves. They also enable to identify typical modal effects such as a modal degeneracy [10] and a localization of modes [11].

In the paper, the modal expansion method is used to predict a low-frequency sound field in rooms with complex-valued boundary conditions on walls. A theoretical modeling is accompanied with a numerical simulation performed for a rectangular enclosure with uniform and frequency constant impedance on room walls. Based on calculation results, the effect of complex wall impedance on a distribution of a pressure

amplitude is investigated and changes in the room transfer function with this impedance are analyzed.

2. Theoretical model

In a low-frequency range, room dimensions are comparable with a length of sound wave and the method, which is most appropriate for determining an interior sound field, is a modal analysis. According to this method, the room response can be described as a superposition of responses of acoustic modes excited in a room by a sound source, i.e.,

$$p(\mathbf{r},t)=\sum_{m=1}^{\infty} p_m(t)\Phi_m(\mathbf{r}), \tag{1}$$

where $\mathbf{r}=(x,y,z)$ is the position coordinate of a receiver, the functions p_m determine a temporal behavior of the sound pressure and Φ_m are the real-valued eigenfunctions which satisfy the orthonormal property in the volume V of the room. In a theoretical model it is assumed that room walls are covered by a sound absorbing material with a complex impedance, thus, the pressure p fulfills the following boundary condition

$$\nabla p\cdot\mathbf{n}=-\frac{1}{c\zeta}\frac{\partial p}{\partial t}, \tag{2}$$

where ∇ is the nabla vector operator, $\mathbf{n}$ is the unit vector normal to the walls, which is directed away from the room volume, and c is the sound speed. In Eq. (2) the quantity ζ represents the specific impedance of a wall material and $\zeta=\zeta_r+\mathrm{j}\zeta_i$, where ζ_r and ζ_i are a wall resistance and a wall reactance, respectively. It is assumed that the magnitude $|\zeta|$ of the wall impedance is much larger than unity because typical materials covering room walls are characterized by a small sound absorption in the low-frequency range [12].

The procedure for finding the function p_m relies on a suitable solution of a wave equation and using the method presented in [13], it can be shown that for small sound damping in a room the function p_m is a solution of the following equation

$$\frac{\partial^2 p_m}{\partial t^2}+2\xi_m\frac{\partial p_m}{\partial t}+\omega_m^2 p_m=c^2\int_V q(\mathbf{r}',t)\Phi_m(\mathbf{r}')\,\mathrm{d}^3\mathbf{r}', \tag{3}$$

where ω_m is the natural eigenfrequency, q is the volume source term in the wave equation, $\mathrm{d}^3\mathbf{r}'=\mathrm{d}x'\mathrm{d}y'\mathrm{d}z'$ is the volume element and the parameter ξ_m is given by

$$\xi_m=r_m+\mathrm{j}\varphi_m=\int_S\frac{(\zeta_r-\mathrm{j}\zeta_i)\Phi_m^2(\mathbf{r})}{|\zeta|^2}\,\mathrm{d}^2\mathbf{r}, \tag{4}$$

where S is the surface area of room walls and $\mathrm{d}^2\mathbf{r}$ is the surface element. Since the wall resistance ζ_r is non-negative, the parameter r_m represents the modal damping factor.

The impulse room response corresponds to the case of an impulsive temporal excitation of a room by a sound source located at a point. Thus, assuming that the volume source term in Eq. (3) has the form $q(\mathbf{r}',\mathrm{t})=\delta(\mathbf{r}'-\mathbf{r}_0)\delta(t-t_0)$ one can obtain

$$\frac{\partial^2 p_m}{\partial t^2} + 2\xi_m \frac{\partial p_m}{\partial t} + \omega_m^2 p_m = c^2 \delta(t - t_0) \Phi_m(\mathbf{r}_0), \tag{5}$$

where $\mathbf{r}_0 = (x_0, y_0, z_0)$ is the source position and t_0 is the time of impulse generation. A method for resolving Eq. (5) was described in [14] and the obtained result is as follows

$$p_m(t) = \frac{c^2 e^{-\xi_m (t - t_0)} \sin[\Omega_m (t - t_0)] \Phi_m(\mathbf{r}_0)}{\Omega_m}, \tag{6}$$

where Ω_m is the complex eigenfrequency for damped modal vibrations given by

$$\Omega_m = a_m + \mathrm{j} b_m = \sqrt{\frac{c_m + \sqrt{c_m^2 + d_m^2}}{2}} + \mathrm{j} \sqrt{\frac{-c_m + \sqrt{c_m^2 + d_m^2}}{2}} \tag{7}$$

where the quantities c_m and d_m are determined by

$$c_m = \omega_m^2 - r_m^2 + \varphi_m^2, \tag{8}$$

$$d_m = 2 r_m \varphi_m. \tag{9}$$

A substitution of Eq. (6) into Eq. (1) leads to the function of the form

$$h(\mathbf{r}_0, \mathbf{r}, t) = c^2 \sum_{m=1}^{\infty} \frac{e^{-\xi_m t} \sin(\Omega_m t) \Phi_m(\mathbf{r}_0) \Phi_m(\mathbf{r})}{\Omega_m} \tag{10}$$

describing the room impulse response (RIR) between the sound source at the position $\mathbf{r}_0$ and the receiver located at the point $\mathbf{r}$. Because of the causality condition, the RIR function $h(\mathbf{r}_0, \mathbf{r}, t)$ is zero for $t < 0$. It satisfies also the reciprocity principle because the right side of Eq. (10) is a symmetric function of the source and receiver points coordinates.

The room impulse response is very useful in room acoustics because a knowledge of the RIR function enables to predict the room response to any sound source. In fact, when a volume source in the wave equation is described by the source function q, the pressure response to this excitation can be found from the following expressions [15]

$$p(\mathbf{r}, t) = \int_V q(\mathbf{r}', t) * h(\mathbf{r}', \mathbf{r}, t) \, \mathrm{d}^3 \mathbf{r}' = \int_V \int_{-\infty}^{t} q(\mathbf{r}', \tau) \, h(\mathbf{r}', \mathbf{r}, t - \tau) \, \mathrm{d}\tau \, \mathrm{d}^3 \mathbf{r}', \tag{11}$$

where the asterisks denotes a convolution operation. The steady-state room response to a point source can be found assuming that in Eq. (11) the source function q takes the form

$$q(\mathbf{r}', t) = Q \delta(\mathbf{r}' - \mathbf{r}_0) e^{\mathrm{j}\omega t}, \tag{12}$$

where ω is the angular source frequency and the amplitude Q of a sound excitation is dependent on the source power W according to the formula $Q = \sqrt{8\pi\rho c W}$, where ρ is the air density. Thus, after performing the volume and time integrations in Eq. (11), a formula for the steady-state sound pressure is found to be as follows

$$p(\mathbf{r}, t) = P(\mathbf{r}) e^{\mathrm{j}[\omega t + \phi(\mathbf{r})]}, \tag{13}$$

where P is the steady-state pressure amplitude

$$P(\mathbf{r}) = \sqrt{\left[\sum_{m=1}^{\infty} \alpha_m \Phi_m(\mathbf{r})\right]^2 + \left[\sum_{m=1}^{\infty} \beta_m \Phi_m(\mathbf{r})\right]^2}, \tag{14}$$

ϕ is the pressure phase given by

$$\phi(\mathbf{r}) = \arctan\left[\frac{\sum_{m=1}^{\infty} \beta_m \Phi_m(\mathbf{r})}{\sum_{m=1}^{\infty} \alpha_m \Phi_m(\mathbf{r})}\right] \tag{15}$$

and the quantities α_m and β_m are determined by

$$\alpha_m = \frac{Qc^2\left[r_m^2 + a_m^2 - b_m^2 - (\omega + \varphi_m)^2\right]\Phi_m(\mathbf{r}_0)}{\left[(r_m + b_m)^2 + (\omega + \varphi_m - a_m)^2\right]\left[(r_m - b_m)^2 + (\omega + \varphi_m + a_m)^2\right]}, \tag{16}$$

$$\beta_m = \frac{-2Qc^2\left[r_m(\omega + \varphi_m) + a_m b_m\right]\Phi_m(\mathbf{r}_0)}{\left[(r_m + b_m)^2 + (\omega + \varphi_m - a_m)^2\right]\left[(r_m - b_m)^2 + (\omega + \varphi_m + a_m)^2\right]}. \tag{17}$$

As it results from Eqs. (14), (16) and (17), the amplitude P is dependent on the source position $\mathbf{r}_0$ and the source frequency ω and, through the quantities a_m, b_m, r_m, and φ_m on the natural eigenfrequency ω_m as well as the real and imaginary parts of the specific wall impedance ζ. Thus, for constant $\mathbf{r}_0$ and given source frequency ω, Eq. (14) enables one to predict a spatial distribution the steady-state pressure amplitude for different values of ζ_r and ζ_i. On the other hand, when the source and observation coordinates $\mathbf{r}_0$ and $\mathbf{r}$ are specified, Eq. (14) makes possible to determine the low-frequency room transfer function for various values of ζ_r and ζ_i at a given point of the room.

3. Analysis of simulation results and conclusions

In the first part of a numerical study, an influence of the absorbing material impedance on a spatial distribution of the steady-state pressure amplitude will be investigated. In general, the developed theoretical model is valid for arbitrary room shapes. However, to perform numerical tests for wider frequency range, a rectangular enclosure is considered because modal vibrations in such a room are well understood and described. The room has the dimensions: $l_x = 7$ m, $l_y = 5$ m, $l_z = 3$ m, and its walls are covered uniformly by an absorbing material with frequency constant complex impedance ζ. Since a small sound damping on room walls is considered, the eigenfunctions Φ_m occurring in Eqs. (14)–(17) were approximated by the mode shape functions for rigid room walls

$$\Phi_m(x,y,z) = \sqrt{\frac{\varepsilon_x \varepsilon_y \varepsilon_z}{V}} \cos\left(\frac{n_x \pi x}{l_x}\right) \cos\left(\frac{n_y \pi y}{l_y}\right) \cos\left(\frac{n_z \pi z}{l_z}\right), \tag{18}$$

where the modal indices n_x, n_y, n_z are non-negative integers and they are not simultaneously equal to zero (the trivial solution of the wave equation was excluded) and $\varepsilon_s = 1$ if $n_s = 0$, $\varepsilon_s = 2$ if $n_s > 0$. The room was excited by the point source with the power W of $1.5 \cdot 10^{-2}$ W located at the position: $x_0 = 5$ m, $y_0 = 3.5$ m, $z_0 = 1.6$ m.

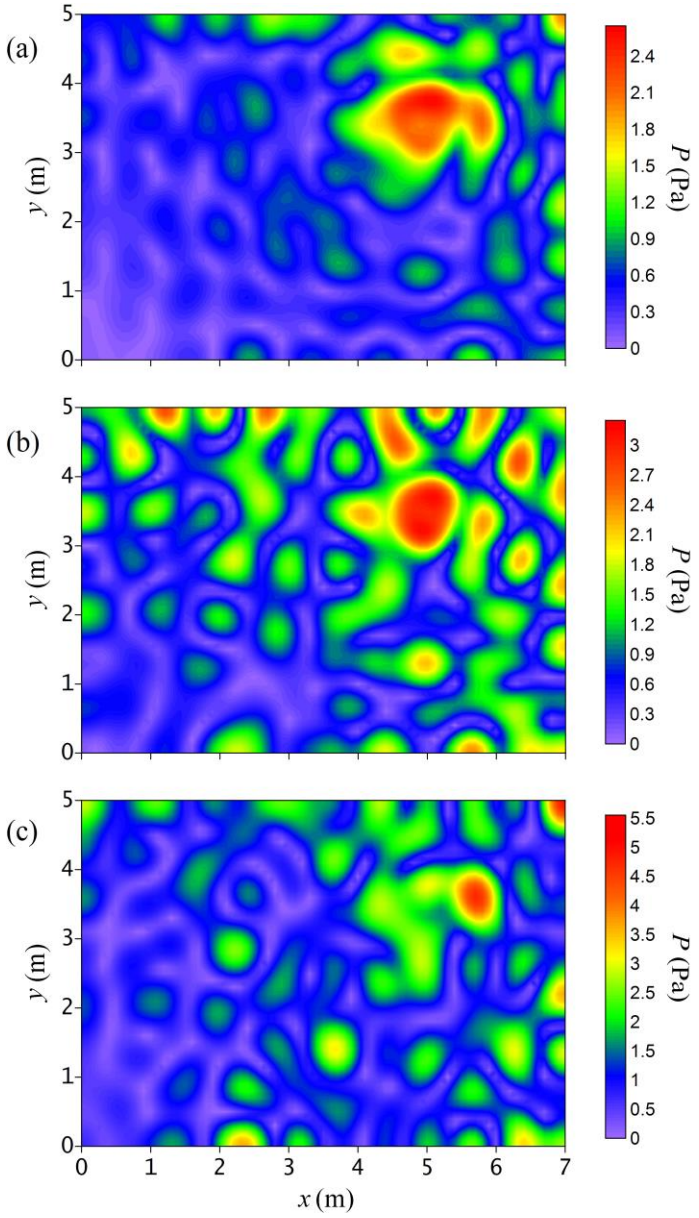

Figure 1. Mapped distribution of the steady-state pressure amplitude P on the (x,y) plane at a distance $z = 1.2$ m from a room floor for the source frequency of 300 Hz and the wall impedance: (a) $\zeta = 10$, (b) $\zeta = 10 + j15$, (c) $\zeta = 10 - j15$

In a numerical algorithm, the room volume was discretized by a mesh system that has uniform horizontal and vertical mesh sizes $\Delta x = \Delta y = \Delta z = 0.05$ m and to predict the steady-state pressure amplitude, Eqs. (14), (16) and (17) were applied. The number of modes included in series in Eq. (14) is an important parameter in a numerical procedure because it greatly influences the simulation accuracy and calculation time. This number depends on room dimensions and it can be approximated from the formula [12]

$$M = \frac{4\pi V}{3}\left(\frac{f_c}{c}\right)^3 + \frac{\pi S}{4}\left(\frac{f_c}{c}\right)^2 + \frac{L}{8}\left(\frac{f_c}{c}\right), \tag{19}$$

where $V = l_x l_y l_z$ is the room volume, $S = 2(l_x l_y + l_x l_z + l_y l_z)$ is the surface of room walls and $L = 4(l_x + l_y + l_z)$ is the sum of the lengths of the room edges. Equation (19) indicates that approximately M modal frequencies are located in the frequency range up to the cutoff frequency f_c. In a numerical simulation it was assumed that $f_c = 600$ Hz, then after inserting this value into Eq. (19) one can obtain $M = 2712$.

Figure 1 shows exemplary simulation results obtained for the source frequency of 300 Hz. The graphs have a form of colored contour maps which are a two-dimensional representation of three-dimensional data. They illustrate a distribution of the steady-state pressure amplitude P on the observation plane $z = 1.2$ m for three different wall impedances: $\zeta = 10$ (Fig. 1(a)), $\zeta = 10 + \mathrm{j}15$ (Fig. 1(b)) and $\zeta = 10 - \mathrm{j}15$ (Fig. 1(c)). The data in Fig. 1 allow us to conclude that the use of absorbing material with non-zero reactance substantially modifies a spatial sound pressure distribution. This is mainly due to the influence of the reactance on damping properties of the absorbing material. These properties are best characterized by means of the random-incident absorption coefficient, which for the complex wall impedance, is expressed by the formula [12]

$$\alpha = \frac{8\zeta_r}{|\zeta|^2}\left[1 - \frac{\zeta_r}{|\zeta|^2}\ln\left(1 + 2\zeta_r + |\zeta|^2\right) + \frac{\zeta_r}{\zeta_i}\arctan\left(\frac{\zeta_i}{1+\zeta_r}\right)\right]. \tag{20}$$

How to check it easily, the coefficient α for the first wall impedance has the value of 0.489, and for two remaining impedances it amounts to 0.217. This explains why for non-zero reactance a maximal value of the amplitude P is larger than in the case of a real-valued wall impedance. It is surprising, however, that for the negative reactance this maximum is about 1.6 times higher than for the positive reactance. This is due to the fact that for the negative reactance the phases φ_m change the sign, thus affecting values of the parameters α_m and β_m used to calculate the pressure amplitude P (Eqs. (16) and (17)).

The second part of the numerical study aims to investigate how the wall impedance affects the low-frequency room transfer function (RTF). Calculations of RTFs were carried out for the receiving point: $x = 2$ m, $y = 3$ m, $z = 1.2$ m, for previously assumed wall impedances. The results are depicted in Fig. 2 and they illustrate frequency dependence of the level L of the pressure amplitude P in the frequency range 50–500 Hz. In Fig. 2(a) the RTFs obtained for $\zeta = 10$ and $\zeta = 10 + \mathrm{j}15$ are presented and they prove that a modal structure of the sound field is better reproduced for non-zero reactance because in this case the room walls provide a smaller sound damping. In Fig. 2(b) the RTFs predicted for $\zeta = 10 + \mathrm{j}15$ and $\zeta = 10 - \mathrm{j}15$ are compared. The interesting thing is

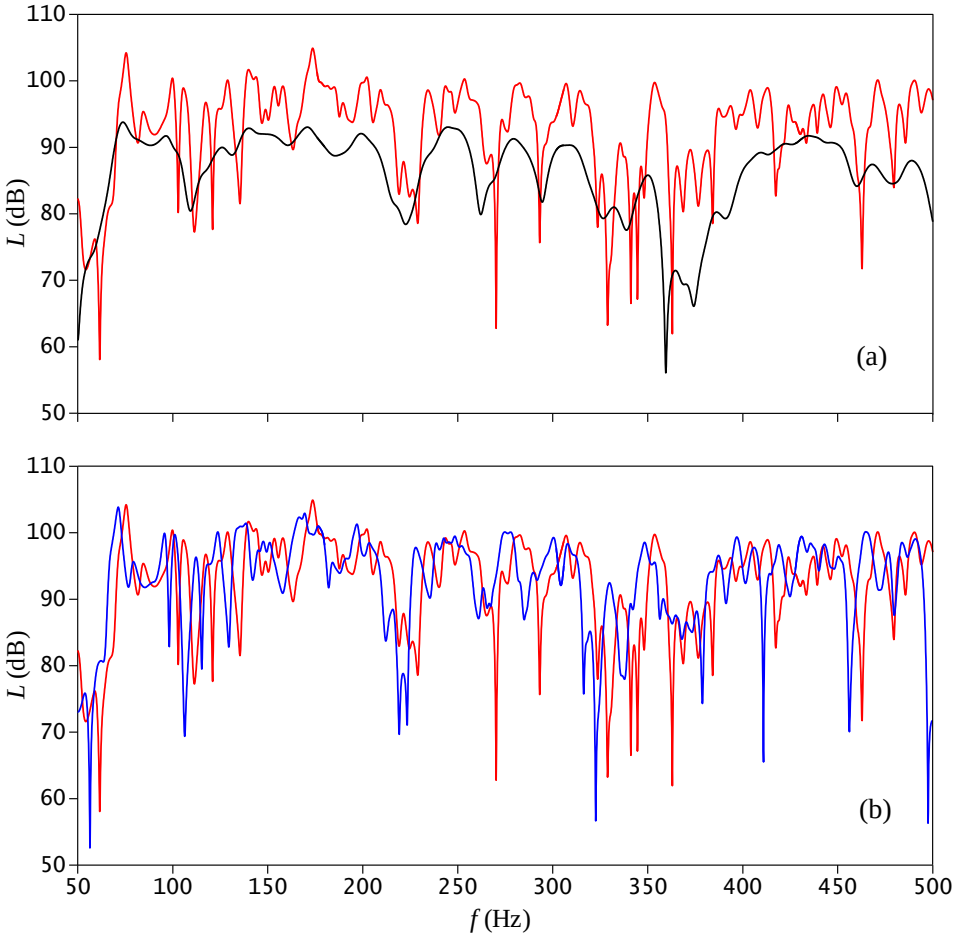

Figure 2. Comparison of the room transfer functions predicted at the observation point: $x = 2$ m, $y = 3$ m, $z = 1.2$ m, for wall impedances: $\zeta = 10$ (black line), $\zeta = 10 + j15$ (red line), $\zeta = 10 - j15$ (blue line)

that the RTFs are shifted about 4 Hz to each other. It results from the fact that in Eqs. (16) and (17) the phase φ_m is always summed with the sound frequency ω, therefore the change of phase sign results in the observed frequency shift.

Acknowledgments

This work was financially supported by the National Science Center, Poland under the project no. 2016/21/B/ST8/02427.

References

1. V. Valeau, J. Picaut, M. Hodgson, *On the use of a diffusion equation for room-acoustic prediction*, Journal of the Acoustical Society of America, **119**(3) (2006) 1504 – 1513.
2. J. Summers, R. Torres, Y. Shimizu, B. Dalenbäck, *Adapting a randomized beam-axis-tracing algorithm to modeling of coupled rooms via late-part ray tracing*, Journal of the Acoustical Society of America, **118**(3) (2005) 1491 – 1502.
3. S. Laine, S. Siltanen, T. Lokki, L. Savioja, *Accelerated beam tracing algorithm*, Applied Acoustics, **70**(1) (2009) 172 – 181.
4. M. Aretz, P. Dietrich, M. Vorländer, *Application of the mirror source method for low frequency sound prediction in rectangular rooms*, Acta Acustica united with Acustica, **100**(2) (2014) 306 – 319.
5. T. Okuzono, T. Otsuru, R. Tomiku, N. Okamoto, *A finite-element method using dispersion reduced spline elements for room acoustics simulation*, Applied Acoustics, **79** (2014) 1 – 8.
6. T. Sakuma, Y. Yasuda, *Fast multipole boundary element method for large-scale steady-state sound field analysis. Part I: setup and validation*, Acta Acustica united with Acustica, **88**(4) (2002) 513 – 525.
7. D. Murphy, A. Southern, L. Savioja, *Source excitation strategies for obtaining impulse responses in finite difference time domain room acoustics simulation*, Applied Acoustics, **82** (2014) 6 – 14.
8. S. Dance, G. Van Buuren, *Effects of damping on the low-frequency acoustics of listening rooms based on an analytical model*, Journal of Sound and Vibration, **332**(25) (2013) 6891 – 6904.
9. K. Sum, J. Pan, *Geometrical perturbation of an inclined wall on decay times of acoustic modes in a trapezoidal cavity with an impedance surface*, Journal of the Acoustical Society of America, **120**(6) (2006) 3730 – 3743.
10. M. Meissner, *Computer modelling of coupled spaces: variations of eigenmodes frequency due to a change in coupling area*, Archives of Acoustics, **34**(2) (2009) 157 – 168.
11. M. Meissner, *Spectral characteristics and localization of modes in acoustically coupled enclosures*, Acta Acustica united with Acustica, **95**(2) (2009) 300 – 305.
12. H. Kuttruff, *Room acoustics*, 5th ed., Spon Press, New York, 2009.
13. M. Meissner, *Acoustic energy density distribution and sound intensity vector field inside coupled spaces*, Journal of the Acoustical Society of America, **132**(1) (2012) 228 – 238.
14. M. Meissner, *Prediction of reverberant properties of enclosures via a method employing a modal representation of the room impulse response*, Archives of Acoustics, **41**(1) (2016) 27 – 41.
15. S. Damelin, W. Miller, *The mathematics of signal processing*, Cambridge University Press, New York, 2012.